

An Investigation of the Orographic Precipitation Sensitivities Within a Sophisticated Bulk Microphysical Parameterization in the MM5

Yanguang Zeng, Brian A. Colle*, and Justin Wolfe

Institute for Terrestrial and Planetary Atmospheres, Stony Brook University/SUNY

1. INTRODUCTION

Compared to other forecast parameters, such as geopotential height or temperature, quantitative precipitation forecasts (QPF) have improved less dramatically during the last few decades (Roebber and Bosart 1998). This lack of precipitation forecast improvement in operational models results from the lack of horizontal resolution, spatial and timing errors of convection and uncertainties in moist physical parameterizations.

Precipitation forecasting over mountainous areas is especially difficult since orographic precipitation is controlled by a number of dynamical and microphysical processes. For example, although it is widely known that moist flow ascending a mountain enhances the precipitation along the windward side, the amount and distribution of orographic precipitation is affected by thermodynamic stratification, moisture availability, wind profile above the barrier, and hydrometeor advection and generation rates.

High-resolution model simulations (Colle and Mass 2000) have suggested that the simulated orographic precipitation structures become more realistic with increased model horizontal resolution; however, they suggested that deficiencies in model microphysical parameterizations result in too much precipitation along the windward slope and too little in the lee.

The parameterizations of clouds and precipitation in numerical models depend on fairly sophisticated bulk microphysical parameterizations (BMPs). For the Penn State/NCAR Mesoscale Model (MM5), there are several levels of sophistication in the BMPs from simple warm rain schemes to more complex mixed-phase schemes. A number of recent field studies over orography (MAP, IPEX, and IMPROVE) were designed to better understand orographic precipitation processes (especially the microphysics) and to improve precipitation forecast skill. However, as we evaluate BMPs using this field data, we also need a better understanding of the model BMP sensitivities and how water mass is transferred between the species to generate precipitation. Even though there are hundreds of users of the MM5, there has been little systematic quantitative evaluation of the BMPs. In this paper we discuss important microphysical pathways that contribute to orographic precipitation and explore how various parameters effect precipitation and microphysical processes.

The following questions will be addressed in this study:

- What are the important microphysical processes and pathways for orographic precipitation?
- What parameters in BMPs lead to the largest sensitivities in surface precipitation and why?
- How are the results applicable to other flow, stability, barrier configurations, and freezing levels?

2. MODEL AND METHODS

This study uses a two-dimensional version of the MM5 to investigate the BMP microphysical sensitivities for a well documented case during the Sierra project on 12 February 1986 (Rauber 1992). This case (hereafter CA86) has served as a benchmark to evaluate the microphysics for the Regional Atmospheric Modeling System (Meyers and Cotton 1992, hereafter referred to as MC92), but there has been no equivalent evaluation of the MM5.

The 2-D MM5 was run nonhydrostatically with 39 sigma levels (terrain-following coordinate) for a 1000 km wide domain. Figure 1a shows a diagram of the profile of the Sierra and coastal range topography smoothed for a 4-km MM5 grid spacing domain. The default

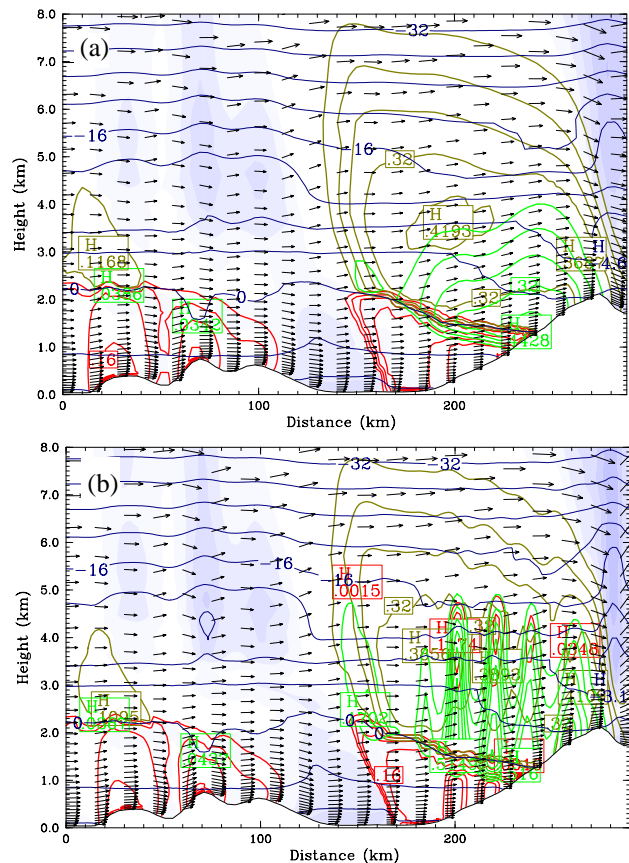


Figure 1. Cross section at (a) 4-km and (b) 2-km grid spacing at hour 6 showing the mixing ratios of snow (dark yellow every 0.08 g kg^{-1}), graupel (green every 0.08 g kg^{-1}), and rain (red every 0.04 g kg^{-1}). Wind vectors, temperature (blue every $4 \text{ }^\circ\text{C}$), and relative humidity (shaded with 100% white) are also shown.

*Corresponding author address: Dr. Brian A. Colle, Marine Sciences Research Center, Stony Brook University, Stony Brook, NY 11794-5000. email: bcolle@notes.cc.sunysb.edu.

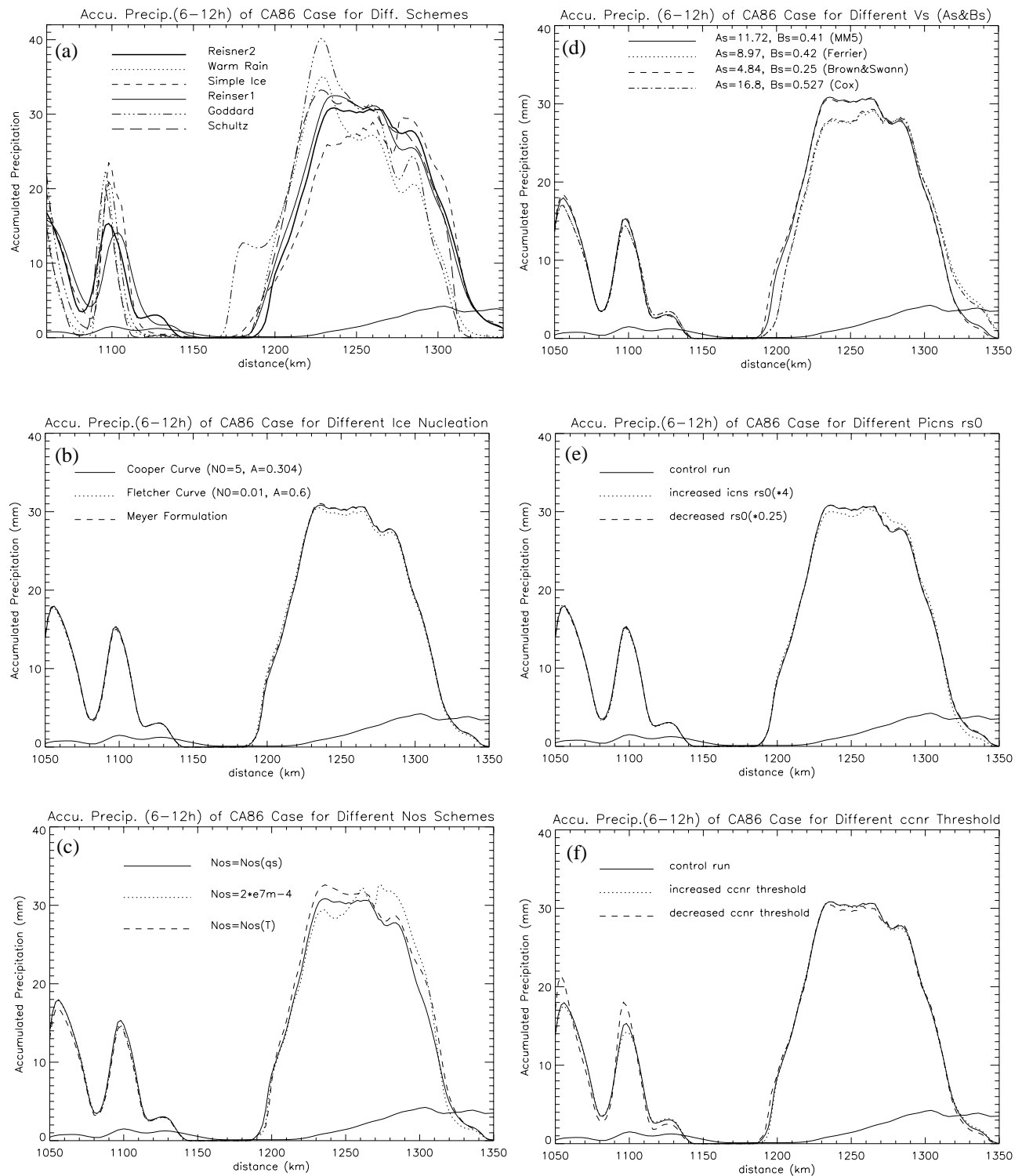


Figure 2. Accumulated model precipitation in mm (6-12 h) versus distance for experiments using different (a) microphysical schemes, (b) ice initiation, (c) snow intercept for snow, (d) snow fall speed, (e) ice to snow autoconversion, and (f) cloud water to rain autoconversion. The terrain profile is also plotted for reference.

microphysical parameterization used is the Reisner2 scheme (Reisner et al. 1998) and no convective parameterization was applied. The MRF scheme was used for planetary boundary layer (PBL), but no heat and moisture surface fluxes were applied. Klemp and Durran (1983)'s upper-radiative boundary condition and a sponge layer were used at the model top to prevent gravity waves from being reflected.

As in MC92, the thermodynamic and moisture profile used to initialize the MM5 is from Sheridan, California on 1500 UTC 12 February 1986 (cf. Fig. 3 of MC92). There was a saturated layer extending up to 2.5 km ASL, while a potentially unstable layer ($d\theta_e/dz < 0$) was situated from 2 to 4 km. The model winds were initialized using the zonal geostrophic component as inferred from the National Centers for Environmental Prediction (NCEP) synoptic charts at 1200 UTC 12 February, since this approach produces a more dynamically consistent flow at start the simulation (MC92).

First, it needed to be determined what horizontal resolution should be used for the simulations. Experiments were run using the same 4-km resolution terrain, but the model grid spacing was decreased incrementally from 4- to 2- to 1.33-km grid spacing. Figure 1 compares cross sections of snow, graupel, and rain for hour 6 of the simulation at 4- and 2-km grid spacing. At 4-km grid spacing (Fig. 1a), there is no evidence of embedded convection within the orographic cloud, while at 2-km grid spacing (Fig. 1b), there are shallow convective plumes of mainly graupel extending up to 4-km. The increase in horizontal resolution resulted in about a 10% increase in surface precipitation over the lower windward slope (not shown). The 1.3-km simulation resolves several more finer-scale convective cores within the potentially unstable layer (not shown). These results suggest that even for a relatively broad barrier such as the Sierras (half width about 50 km), 4-km grid spacing is not sufficient to realistically simulate the embedded convection within the larger orographic cloud. Since the 2-km grid captured the salient aspects of this convection, this resolution was used for the remaining sensitivity studies.

3. SIERRA CA86 2-D SIMULATIONS

For the CA86 case, several different MM5 microphysical parameterizations were tested as well as several parameters within the Reisner2 scheme.

a. Different microphysical schemes.

Five MM5 microphysical schemes (warm rain, simple ice, Reisner1, Goddard and Schultz) were compared to the Reisner2 scheme (the control run) for a 12-h simulation at 2-km grid spacing. Figure 2a shows the 6-12 h surface precipitation distribution for the different BMPs.

The warm rain and Goddard schemes produce the largest precipitation amounts along the lower windward slope (25-50% more than the Reisner2 scheme) and much less along the upper windward slope. Without ice in the warm rain scheme or a well-defined snow field in the Goddard (Fig. 3), more water vapor condenses to cloud water, autoconverts to rain, and precipitates rapidly over the lower windward slope. Without super-cooled water and graupel in the simple ice scheme there is about 10-30% less precipitation along lower and mid windward slope than the other schemes. The lack of super-cooled water and a fixed slope intercept for snow number con-

centration in the simple ice results in twice as much snow mass aloft than the Reisner2 (Fig. 3). This extra snow in the simple ice advects downwind and results in about 20% more precipitation over the crest. The simple ice scheme also produces more rain over the coastal range, which suggests that it has a large precipitation efficiency for this narrow barrier (not shown). The Reisner1 precipitation and snow field are similar to Reisner2 (not shown), since both use a variable Nos as a function of rain/snow rate. However, Reisner1 produces slightly more precipitation over the lower windward slope and less near the crest than the Reisner2 (less than 10%). These differences may result from fixed rain intercept used in Reisner1, different autoconversion thresholds from cloud water to rainwater or cloud ice to snow, and different ice deposition expressions. The Schultz scheme includes super-cooled water, ice, and graupel, but the results are similar to the warm rain scheme, with a peak of precipitation at the base of the windward slope and less precipitation in the lee than other schemes. There is much more cloud ice and much less snow over the windward side in the Schultz than Reisner2 (not shown), since the threshold from cloud ice to snow is much larger than the Reisner2 scheme.

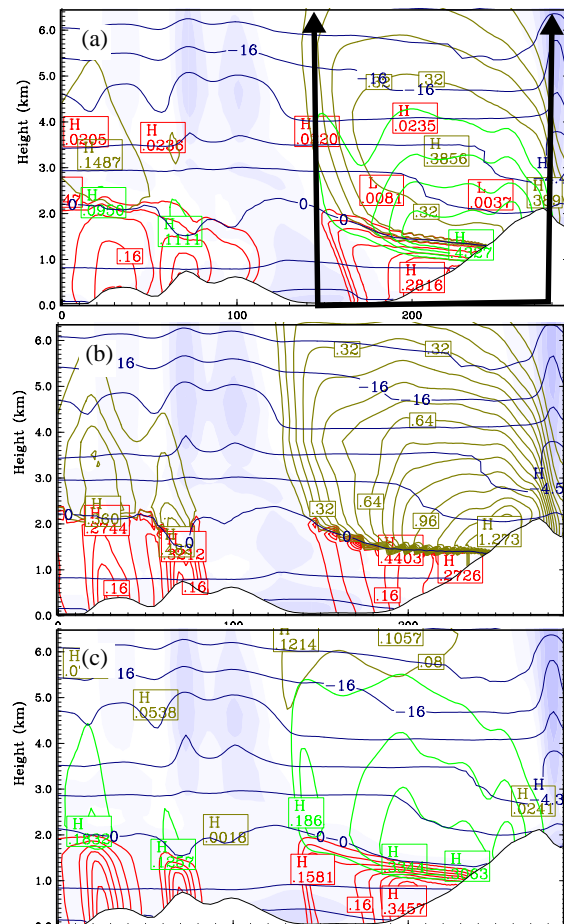


Figure 3. Cross section for the (a) Reisner2, (b) simple ice, and (c) Goddard MM5 BMPs averaged for 6-12 h at 2-km grid spacing showing the mixing ratios of snow (dark yellow every 0.08 g kg^{-1}), graupel (green every 0.08 g kg^{-1}), and rain (red every 0.04 g kg^{-1}). Wind vectors, temperature (blue every $4 \text{ }^\circ\text{C}$), and relative humidity (shaded with 100% white) are also shown. The boxed region in (a) is where the microphysical budget is calculated.

b. Reisner2 sensitivities

Several experiments were completed to test the sensitivity of the Reisner2 BMP to changes in ice initiation, Nos, snow fallspeed, and autoconversions of cloud water and ice.

Initiation of primary and secondary ice processes are important to simulate the various water and ice species (cloud water, graupel and snow aggregates), as well as the radiative properties of clouds. In fact, without ice initiation to seed the cloud, there would be no snow aloft in the model, so it represents an important pathway to generate surface precipitation. There are several ice initiation schemes available, such as Fletcher (1962), Meyers and Cotton (1992), and Cooper (1986). These three schemes were tested for the CA86 case. Interestingly although ice initiation is an important pathway for snow, there is little sensitivity to the surface precipitation (Fig. 2b). The Fletcher tends to produce more cloud ice aloft than the other schemes (not shown), but the snow fields are nearly identical in all experiments (not shown). This suggests that only a portion of this ice is needed to create a snow field that grows rapidly via deposition and accretion.

Nos, the slope intercept in the Marshall-Palmer distribution for snow, is not only important in the snow fall speed calculation, which can affect not only snow amounts aloft and the surface precipitation, but also the collection, deposition and melting of snow. Reisner et al. (1998) compared fixed Nos with a variable Nos expression as a function of snow rate, and found that fixed Nos depleted too much cloud water. To further examine the effect of Nos on microphysical processes and the surface precipitation, the snow intercept parameter Nos was changed to either a fixed value ($Nos = 2 \times 10^7 \text{ m}^{-4}$) or temperature dependent Nos (Houze 1979). Varying Nos results in a 10-15% change in the surface precipitation. Specifically, a fixed Nos, such as in the simple ice scheme, results in more snow aloft and a shift of surface precipitation from the lower windward slope to the crest. In contrast, for the coastal range, there is little sensitivity to Nos. This is consistent with the shorter time that snow has to grow crossing this narrow mountain, which results in little snow aloft.

Four different relationships were tested for the snow fallspeed. The Cox (1988) and Ferrier (1994) fallspeeds are on average 20-30% slower than the control MM5 (not shown). As a result, the precipitation maximum shifts from the lower windward slope to the crest, resulting in 10-20% less precipitation over the lower windward slope. The slower fallspeed also results in 30-40% more precipitation in lee of the Sierras. In contrast, there is little sensitivity over the coastal range, which is consistent with the limited snow over this narrow barrier.

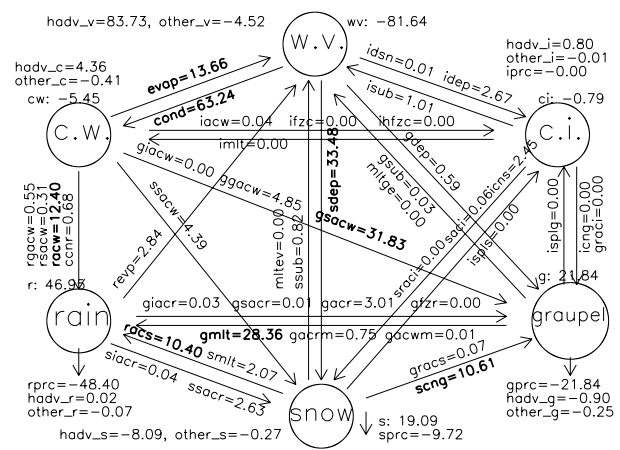
The MM5 converts cloud ice to snow at relatively small sizes (150 μm diameter). As a result, there is very little water mass in the cloud ice category as compared to snow (0.10 g/kg versus 0.60 g/kg for snow). The separation between cloud ice and snow can have an effect on what processes each species interacts with and their fallspeeds. When the maximum size was increased by a factor of four, there was more suspended cloud ice, which resulted in slightly more precipitation near the crest compared to the windward slope. There was no impact in reducing the maximum cloud ice threshold.

There was also little impact on the surface precipitation over the Sierras when doubling or halving the autoconversion threshold of cloud water to rainwater (0.35 g kg^{-1} in CTL). This is consistent with most of the precipitation being produced as snow/graupel over the Sierras. In contrast, there is more sensitivity to this autoconversion for the narrower coastal range, since the stronger upward motion results in low-level maximum of cloud water (not shown).

4. MICROPHYSICAL BUDGET

For a box upstream of the Sierra Mountain crest (shown in Fig. 3a), a microphysical budget was calculated. Each microphysical process rate is averaged over this box from 6 to 12 hours. The process values are normalized by the water vapor loss rate. The abbreviated names of the processes in the budget are the standard ones used, such as in Reisner et al. (1998).

Budget Flowchart of CA86 Case (6–12h) of the Control Run*



*Budget Flowchart Diff. with Run1 of CA86 Case for Fixed Nos**

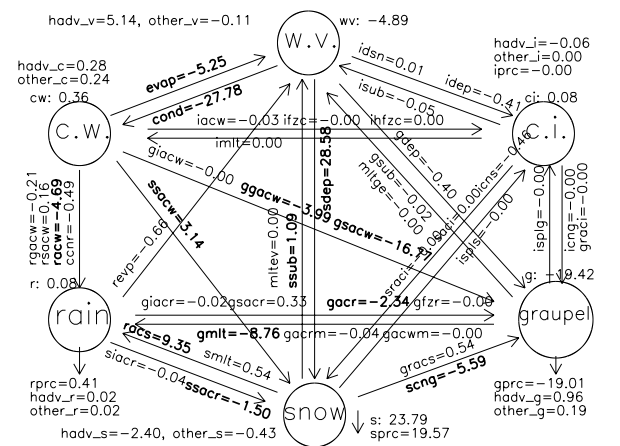


Figure 4. (a) Microphysical budget for the Reisner 2 control run averaged over the box in Fig. 3a for the 6-12 hour period. The process rates are normalized by the water vapor loss rate, and the arrows point in the direction of the water/ice movement. The bold numbers are values greater than 10% of the water vapor loss rate. (b) Same as (a) except for the difference between the fixed Nos experiment and the control (Fixed Nos - CTL). Absolute differences greater than 2.0 are bold.

Figure 6a shows the microphysical flowchart of the control run over the barrier, with values greater than 10% highlighted in bold. There are two important pathways that contribute to surface precipitation. First, cloud water forms via vapor condensation ($\text{cond}=63.24\%$), then converts to graupel through riming of cloud water onto graupel ($\text{gsacw}=31.83\%$) at temperatures colder than 0°C , or converts to rain via collection of cloud water ($\text{racw}=12.40\%$) at warmer temperatures. Second, snow forms directly from deposition of water vapor ($\text{sdep}=33.48\%$). Furthermore, melting of graupel ($\text{gmelt}=28.36\%$), accretion of cloud water by rain ($\text{racw}=12.40\%$) and collection of snow by rain ($\text{racs}=10.40\%$) are also important sources of rain.

Figure 6b compares the control microphysical processes with the experiment using a fixed Nos for snow. A fixed Nos changes the microphysical pathways dramatically. The amount of snow deposition (sdep) doubles compared to the control. There is much less condensation, cloud water and conversion to graupel with the fixed Nos. Therefore, snowfall contributes much more to the fallout of surface precipitation over the windward slope rather than graupel, which is similar to the simple ice solution (Fig 3b). Using a temperature dependent Nos also results in less cloud water and graupel (not shown), but the pathways changes are only half as large as the fixed Nos experiment.

5. 2-D IDEALIZED RUNS

In this section we investigate the microphysical sensitivities to barrier width and freezing level. A bell-shaped barrier of 2000 m height was used, with a mountain half width of 10 km or 50 km. A moist static stability (N_m) of 0.005 s^{-1} and nearly saturated sounding (99% relative humidity) were used. The freezing level was changed from 750 mb in the control run to 500 mb or 1000 mb in order to investigate the effects of freezing level. The upstream flow is 15 m s^{-1} for all the experiments. The control run for the idealized experiments is a barrier with height of 2000 m, 50-km half width, and 750 mb freezing level, which is similar to the CA86 case.

First, the sensitivity of Nos to barrier width was tested. As in the CA86 case, a fixed Nos for a wide barrier leads to an increase in snow deposition, which results in more snow mass. Less cloud water is created because of less condensation of water vapor, resulting in less collection and autoconversion processes from cloud water to rainwater or graupel. Overall, there is 4 mm (20%) more surface precipitation over the crest (Fig. 5a)

For narrow barrier (10-km half width), the changes in microphysical fields and surface precipitation with fixed Nos are much smaller than for the wide barrier over the windward slope (Fig. 5b, less than 3%). There is less sensitivity since the advection time is shorter for a narrow barrier, resulting in less time for snow to grow and fall out over the windward slope. Other sensitivities involving ice processes such as fallspeeds and ice to snow autoconversion also show less sensitivity for the narrow barrier since there is less ice aloft given the short advection time scales (not shown).

In the CA86 case, there was little sensitivity to autoconversion of cloud water to rain water (ccnr) over the Sierras (Fig. 2e), while there were larger changes for the narrow coastal range. To quantify this further, the sensitivity of ccnr threshold was tested for the idealized wide and narrow barriers. For a wide barrier (Fig. 6a), an

increased ccnr threshold leads to decreased autoconversion, which results in 1.2 mm (5-10%) less surface precipitation due to decreased rain along the lower windward slope. For the narrow barrier (Fig. 6b), there is 4 mm (26%) more surface precipitation over the lower windward side for increased ccnr threshold and 8 mm (20%) less precipitation for decreased ccnr threshold over the upper windward slope. The narrow barrier is also more sensitive to processes involving graupel, such as graupel density or graupel fallspeed, since graupel is favored for a narrow barrier with stronger vertical motions.

When the freezing level is increased from 750 mb to 500 mb, there is less snow or graupel but warm rain processes. More water vapor goes to rain through accretion and autoconversion processes (racw , ccnr) after condensation instead of to snow or graupel by collection processes. With an increased ccnr threshold for a wide barrier, rain is decreased and cloud water is increased, resulting in 6 mm (15%) less surface precipitation along upper windward slope (Fig. 7). A decrease in the ccnr threshold leads to 3 mm (20%) more surface precipitation over lower windward side. Compared with freezing level at 750 mb (Fig. 6a), the differences of ccnr are slightly more apparent with higher freezing level such as 500 mb since higher freezing level allows for more cloud water and less ice. When the freezing level is lowered to 1000 mb (not shown), the sensitivity to ccnr decreases and there is more sensitivity to ice processes, such as

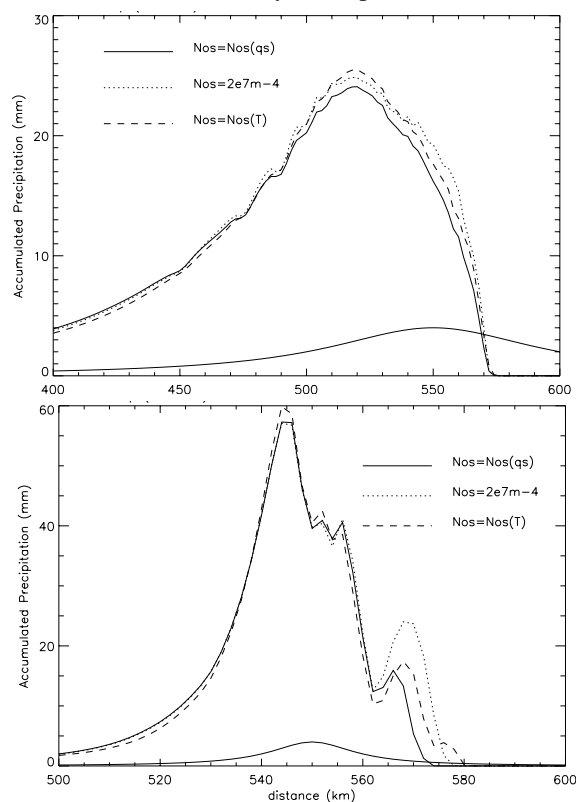


Figure 5. Accumulated model precipitation in mm (6-12 h) versus distance using different snow slope intercepts (Nos) for a relatively (a) wide (50-km half width) and (b) narrow (10-km half width) barrier of 2000 m height.

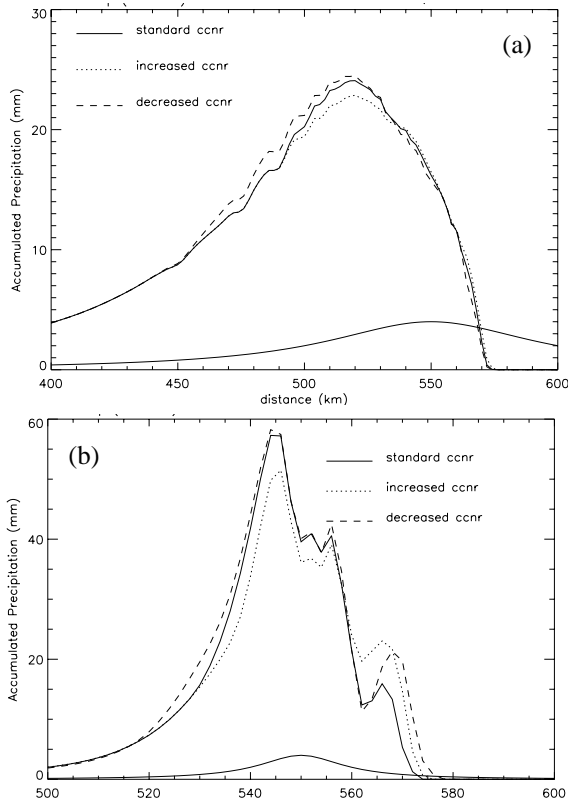


Figure 6. Accumulated model precipitation in mm (6-12 h) versus distance using different cloud water autoconversion thresholds for a relatively (a) wide (50-km half width) and (b) narrow (10-km half width) barrier of 2000 m height.

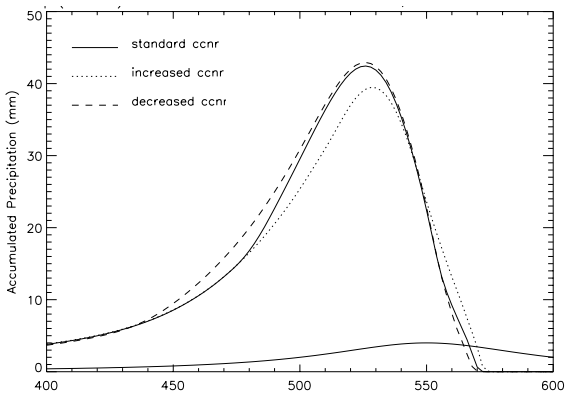


Figure 7. Accumulated model precipitation in mm (6-12 h) versus distance using different cloud water autoconversion thresholds for a relatively wide (50-km half width) barrier and a 500 mb freezing level.

6. SUMMARY

Using a two-dimensional version of the MM5, this studies compared several microphysical schemes and microphysical processes for an orographic precipitation event over the Sierra Mountains on 12 February 1986. This study is similar to that done for the 2-D RAMS model for the same event (MC92). The MM5 simulations illustrate that less than 4-km grid spacing was necessary

to properly simulation the narrow convective plumes associated with a potentially unstable layer around 750 mb.

There was a large spread 30-40% between many of the microphysical schemes for the orographic precipitation, thus illustrating the uncertainty in the current generation of BMPs. Several processes within the Reisner2 BMP were tested, such as slope intercept for snow, fall-speeds, and autoconversions, but none of these processes individually yielded as large of a sensitivity than using a different BMPs. The slope intercept for snow (Nos) and snow fallspeed yielded the largest sensitivity for the CA86 case.

The sensitivity to the microphysical processes are a function of the barrier width and freezing level. In particular, ice-related processing (Nos, ice fallspeeds, autoconversions) are more sensitive for wide barriers such as the Sierras, since the advective time scales are longer. In contrast, for a narrow barrier and higher freezing level, there is more sensitivity to graupel and cloud-water related processes, such as graupel density, fallspeed, and cloud water to rain autoconversion, since the upslope motions are greater, thus creating more cloud water and less ice.

7. ACKNOWLEDGEMENTS

This research is supported by the National Science Foundation (Grant No. ATM-0094524). The 2-D MM5 was developed by Prof. Dave Dempsey and the MMM Division of NCAR.

8. REFERENCES

- Colle, B.A., and C.F. Mass, 2000: The 5-9 February 1996 flooding event over the Pacific Northwest: Sensitivity studies and evaluation of the MM5 precipitation forecasts. *Mon. Wea. Rev.*, **128**, 593-617.
- Cooper, W.A., 1986: Ice initiation in natural clouds. *Precipitation Enhancement a Scientific Challenge, Meteor. Monogr.*, No.21, Amer. Meteor. Soc., 29-32.
- Cox, G.P., 1988: Modeling precipitation in frontal rainbands. *Quart. J. Roy. Meteor. Soc.*, **114**, 115-127.
- Fletcher, N.H., 1962: *Physics of Rain Clouds*. Cambridge University Press, 386 pp.
- Houze, R.A., P.V. Hobbs and P.H. Herzegh, 1979: Size distributions of precipitation particles in frontal clouds. *J. Atmos. Sci.*, **36**, 156-162.
- Meyers, M.P., and W.R. Cotton, 1992: Evaluation of the potential for wintertime quantitative precipitation forecasting over mountainous terrain with an explicit cloud model. Part I: Two-dimensional sensitivity experiments. *J. Appl. Meteor.*, **31**, 26-50.
- Rauber, R.M., 1992: Microphysical structure and evolution of a Sierra Nevada shallow orographic cloud system. *J. Appl. Meteor.*, **31**, 3-24.
- Reisner, J., R.M. Rasmussen, and R.T. Bruintjes, 1998: Explicit forecasting of supercooled liquid water in winter storm using the MM5 mesoscale model. *Quart. J. Roy. Meteor. Soc.*, **124**, 1071-1107.
- Roebber, P. and L.F. Bosart, 1998: The sensitivity of precipitation to circulation details. Part I: An analysis of regional analogs. *Mon. Wea. Rev.*, **126**, 437-455.